JOURNAL OF Applied Polymer SCIENCE

Characterization of Void Formation in Polyamide 6 Under Tensile Creep in Alcohols by Using Thermoporosimetry

Eiichi Sakai,[1] Makoto Kawagoe[2]

[1]Department of Machine Intelligence and Systems Engineering, Faculty of Systems Science and Technology, Akita Prefectural University, 84-4 Tsuchiya-Ebinokuchi, Yurihonjo, Akita 015-0055, Japan

[2]Department of Mechanical Systems Engineering, Faculty of Engineering, Toyama Prefectural University, 5180 Kurokawa, Imizu, Toyama 939-0398, Japan

Correspondence to: E. Sakai (E-mail: e_sakai@akita-pu.ac.jp)

ABSTRACT: The void formation in polyamide 6 under tensile creep in alcohols has been characterized by use of thermoporosimetry. After the specimens were creep-elongated to a common preset strain of 9% in ethanol, 1-propanol, 1-butanol, 1-hexanol, and 1-octanol at room temperature, they were soaked in distilled water at 20°C, and then offered to the differential scanning calorimetry (DSC) under cooling. The exothermic peaks indicating the presence of freezable water were detected for all the specimens elongated in alcohols except 1-octanol. The void size distributions were assessed from the DSC curves by thermoporosimetry. The pores for the ethanol environment showed a wide size distribution from 2.5 to 8.5 nm in radius. The pores for 1-propanol and 1-butanol showed narrower distribution from 3 to 4 nm, and those for 1-hexanol concentrated upon very small size of about 2 nm. The average pore radius was shown to be correlated with the solubility parameter of environmental alcohol. © 2013 Wiley Periodicals, Inc. J. Appl. Polym. Sci. 130: 1595–1601, 2013

KEYWORDS: polyamides; mechanical properties; differential scanning calorimetry (DSC)

Received 29 November 2012; accepted 28 March 2013; Published online 30 April 2013

DOI: 10.1002/app.39335

INTRODUCTION

In semicrystalline polymers, as well known, the large plastic deformation under tensile loading usually introduces the formation and growth of voids.[1–6] According to Friedrich,[1] such a voiding process in deformation is closely related to the formation of craze, the structure of which consists of many elongated fibrils and voids. He has presented a microdeformation mechanism describing the collapse of lamellar structure and void formation leading to the craze on the basis of observations by the scanning electron microscopy (SEM) and the transmission electron microscopy (TEM). Butler et al.[2,3] have conducted precise investigation on the microstructure changes in linear polyethylene by using the technique of simultaneous small-angle X-ray scattering (SAX) during the deformation, directly corresponding to the load-extension curve. They have revealed and discussed, although not referred to the craze, the lamellae fragmentation and the void development (cavitation) in the interlamellar regions to take place in the processes of strain softening after yielding and subsequent cold drawing.

With regard to the analysis of material microstructure including a number of voids, the thermoporosimetry is of great interest.[7–13] This method assesses the pore size distribution in the porous materials usually from the freezing curve of contained water by differential scanning calorimetry (DSC) under cooling. In the thermoporosimetry, the abscissa (temperature) and the ordinate (heat flow) of DSC curve are transformed into the pore radius and the change in the pore volume, respectively, and as a result a spectrum of pore size distribution is obtained. Ishikiriyama et al.[7,8] have precisely developed this method and examined its validity by comparing with the experimental results of nitrogen gas adsorption–desorption and mercury porosimetry for several different silica gels. Their theoretical evaluation was indicated to agree well with the experiments. Other investigators[9–13] also have demonstrated the thermoporosimetry to be successfully useful for evaluating the pore size distributions in several materials, although they have noted that this method may be adequate in the pore size range from approximately 1.8 to 30 nm in radius in principle of capillary condensation of water.[10]

Noting such an effectiveness of thermoporosimetry, the authors[14] have applied this method to the evaluation of microstructure changes with void formation in polyamide 6 (PA6) under quasi-static simple elongation in air. The void (cavity) formation in a plastically deformed PA6 has already been suggested by Galeski et al.[4] through TEM observations. The PA6 is

well known as one of the semicrystalline engineering polymers, and shows hydrophilic characteristic because of the amide group leading to considerable water absorption. Using this property, the PA6 specimens were immersed in distilled water at room temperature after the preliminary elongation to several levels in air, and subsequently subjected to the DSC measurements under cooling. No exothermic signal was obtained for the lightly deformed specimens as well as the nondeformed one, despite a considerable amount of absorbed water. This was interpreted to show that the absorbed water is in a state of nonfreezing bound water[15,16] under the action of hydrogen bonding.[17] On the other hand, a large exothermic peak at about −34.5°C and other small peaks at lower temperatures than distilled bulk water are clearly detected for the highly elongated specimen (just before fracture). These remarkable exothermic peaks were understood to denote that the absorbed water partially exists in a freezable state in the voids formed with the collapse of crystals under higher level of elongation.[1–6] The depression in the freezing temperature of water was transformed into the void size by using the thermoporosimetry. For both models of cylindrical and spherical voids, their size distributions were assessed to have average radii of about 2.5 and 2.7 nm, respectively. These results seem to be reasonable in comparison with the literatures.[5,18,19] Thus the thermoporosimetry may be effective for evaluating the voided polymer microstructure by plastic deformation, although its application is limited to hydrophilic polymers.

In the case of the plastic deformation of polymers, it is also noted that the environmental organic liquids exert great influences in general.[20] However, compared with the noncrystalline (amorphous) polymers, the effects of organic liquid on the plastic deformation of semicrystalline polymers have not been sufficiently examined, particularly with respect to the void formation,[21] even including the studies of environmental stress cracking (crazing) (ESC).[22] The past investigations on the plastic deformation with voiding in semicrystalline polymers[1–6,14] have mainly focused on the behavior in air, as mentioned above. The ESC is of practical importance for causing about 30% of all failures of polymeric products.[23] Therefore the study of void formation in semicrystalline polymers under cooperative actions of tensile stress and organic media like alcohols is significant in relation to the ESC in these polymers.

In view of the above, this article attempts to apply the method of thermoporosimetry based on the DSC freezing behavior of absorbed water to the evaluation of void formation in PA6 during the creep deformation under alcohol environments, as an extension of our previous work.[14] In this article we first report the creep deformation of PA6 under constant tensile loading in five different alcohols, secondly examine the DSC freezing behavior of absorbed water in these creep-deformed specimens, and lastly assess the void size distribution on the basis of thermoporosimetry.

EXPERIMENTAL

Material and Specimen Preparation

The material used in this article was a commercially available PA6 pellet (Ube Industries, Ube Nylon 6, S1013NW8). The molecular weight of PA6 of this grade is unfortunately unknown, because no data are officially announced from the above company, and further any appropriate device for actual measurements was not equipped in our laboratory. As the molecular weight (distribution) is an important factor affecting the mechanical properties of polymer specimen in general, some investigations are desired in future.

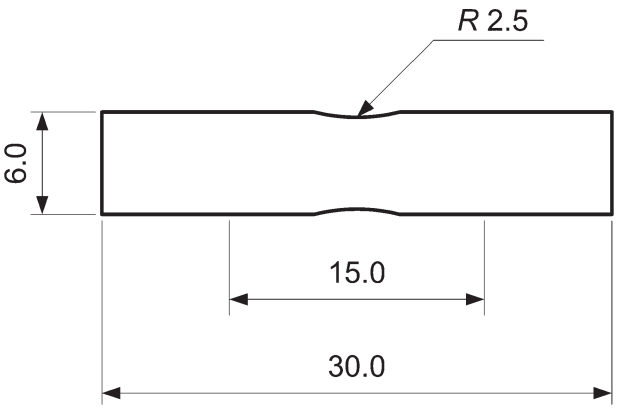

Figure 1. Geometry of specimen 0.5 mm in thickness. Dimensions are in mm.

The pellets were preliminarily dried at 80°C at a lowered pressure of about 9.3 kPa for 3 h in a vacuum chamber (Shibata Scientific Technology, Japan; VOR-300). After the preliminary drying, the pellets of about 8 g filled in a rectangular mold of stainless steel were preheated at 250°C for 4 min, and compressed at about 15 MPa for 3 min by using a hot press equipment (Imoto Machinery, Japan; IMC-180), and then slowly cooled to room temperature at a rate of about 3.3°C/min. The PA6 sheet removed from the mold was cut into the rectangular specimen of 30 × 6 × 0.5 mm with small notches (2.5 mm in radius) on both sides of central part to make a largely deformed zone, which was supplied to the thermal analysis described later. The cut surfaces were polished with abrasive papers of No. 400 and 1000. The specimen geometry is shown in Figure 1. The degree of crystallinity of specimen was evaluated at 33.2% by a densitometry (JIS K7112[24] using an electronic densimeter (Mirage Trading, Japan; SD-200L) and the density data of crystalline (1.23g/cm^3) and amorphous (1.10g/cm^3) phases of PA6 in the literature.[25]

The specimens prepared in the above way were the same as those in the previous work[14] except the dimension of grip parts for bearing the tensile load.

Creep Loading

The tensile creep loading was applied to the specimen in alcohol environment by using a testing machine of our own making with a dead weight-lever loading system and a liquid vessel, as schematically shown in Figure 2. Five kinds of alcohol: ethanol, 1-propanol, 1-butanol, 1-hexanol, and 1-octanol, were used as the environmental reagents. Table I shows their purity[26] and basic properties at room temperature.[27,28] In the table a value of solubility parameter of 2-ehyl-1 butanol (a branched isomer of 1-hexanol) is given instead of that of 1-hexanol, because only this isomer is found even in the reference[28] that seems to

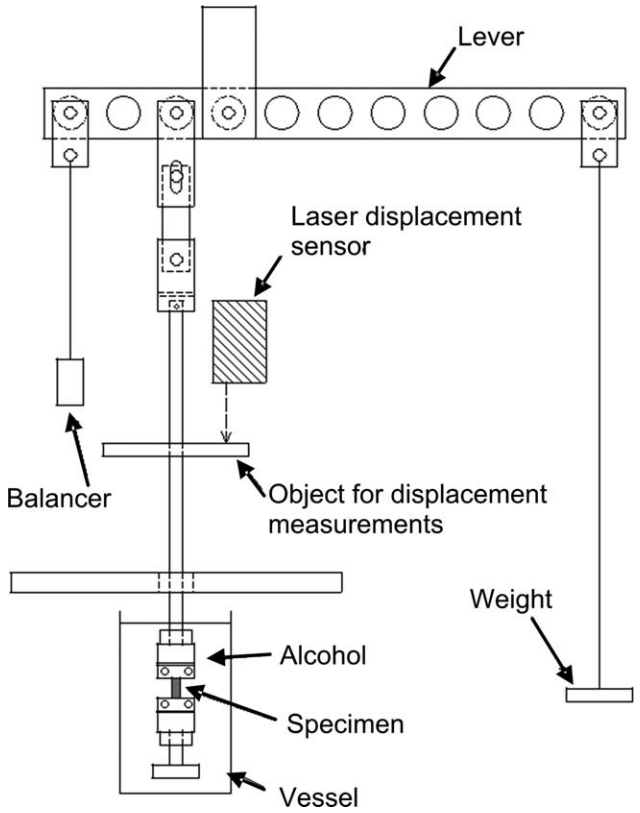

Figure 2. Schematic illustration of the apparatus for creep loading in alcohols.

include the most comprehensive data of solubility parameter. All the specimens were loaded to the same degree of deformation in order to compare mutually the variations in polymer microstructure (void formation) under different alcohol environments. Thus a common tensile load of 112.5 N (nominal stress of 45 MPa) was given to the specimens until reaching the same total elongation of 1.35 mm (nominal strain of 9%), which was determined from a preliminary test in ethanol as the limit of deformation without fracture. The nominal creep strain here was conveniently given by dividing an elongation of specimen by an initial gauge length (distance between the jaws) of 15 mm. The elongation of specimen was monitored by using a laser displacement sensor (Keyence, LB1000) equipped on the testing machine. The temperature of alcohol was held almost constant (~23°C) by conducting the tests in a thermostatically controlled room.

Table I. The Purity[26] and Basic Properties of Alcohols Used as the Environmental Reagents at Room Temperature[27,28]

Alcohol (purity)	Molar volume 10^{-6} m^3/mol)	Solubility parameter ($(MJ/m^3)^{1/2}$)
Ethanol (99.5v/v%)	58.5	26.0
1-propanol (99.5w/w%)	74.8	24.8
1-butanol (99+[a] w/w%)	91.5	23.3
1-hexanol (97+w/w%)	124.8	21.5[b]
1-octanol (98+w/w%)	157.7	21.1

[a] Symbol "+" means the purity above numerical value indicated.[26]
[b] The value of 2-ethyl-1-butanol is given in place of value of 1-hexanol.[28]

DSC Measurements for Water-Soaked Specimens

The rectangular small parts of approximately 15 × 4 × 0.3–0.5 mm were cut from the largely elongated region of above creep-loaded specimens after preliminary drying at 23°C at 9.3 kPa for 18 h in the above-mentioned vacuum chamber. Then they were soaked in a beaker of distilled water at 20°C set in a temperature-controlled oven (Tokyo Rika, Japan; KCL-1000). The weight of specimen was measured by an electronic balance (Mettler-Toledo, Switzerland; AE-240). The water content was calculated from the weight gain against the initial weight of dried specimen. In order to compare properly the thermal behavior of absorbed water in a specimen with the others, the specimens were prepared so as to have almost the same water content, and as a result the amounts of absorbed water were 7.9wt % for the specimen loaded in ethanol and 7.8wt % for the others, respectively.

The water-soaked specimen was further cut into a small circle of about 3 mm diameter, and then sealed in an aluminum pan for the DSC, as quickly as possible for suppressing the water desorption. The DSC measurements were conducted by use of a heat-flow type differential scanning calorimeter (SII Nano Technology, DSC6100) with a cooling device from 20°C to −70°C at a rate of 2.0°C/min. The alumina (Al_2O_3) powder was used as a reference matter.

RESULTS AND DISCUSSION

Creep Behavior

Figure 3 shows the variations of creep strain until 9% with loading time in the test alcohols. As the preliminary experiments using five different specimens for each alcohol showed almost the same results, only one typical creep curve is given for each alcohol in the figure. Irrespective of the kind of environmental alcohol, the creep strains in common show the initial

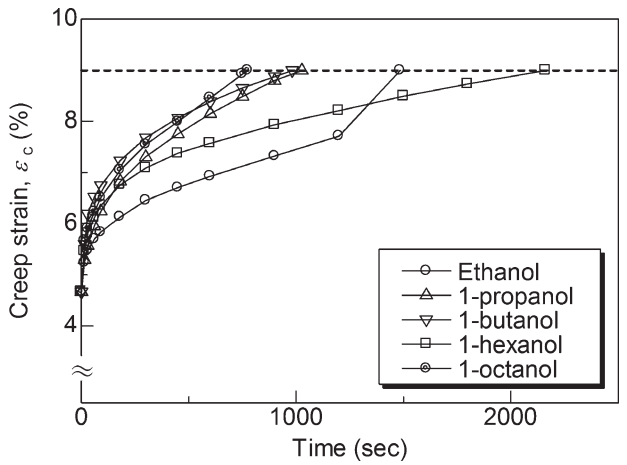

Figure 3. Typical creep curves of the PA6 specimens in five different alcohols.

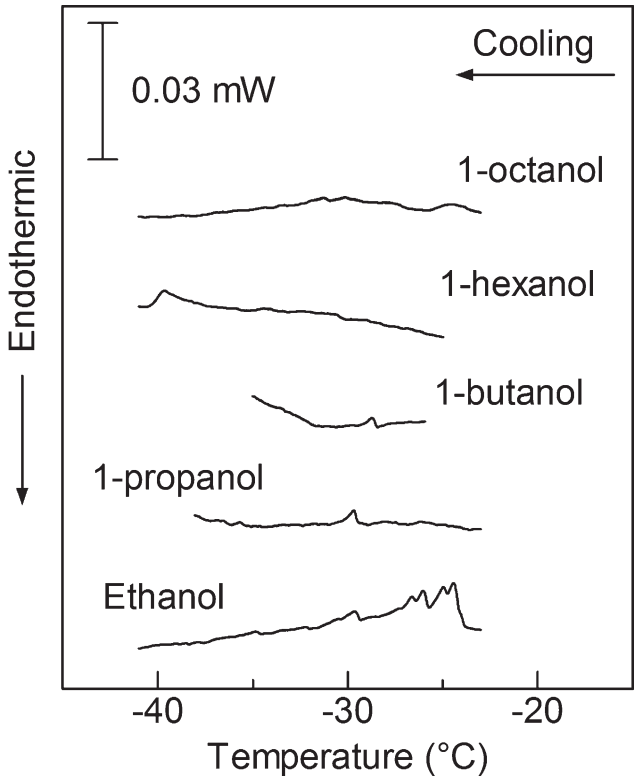

Figure 4. DSC cooling curves of the water-soaked specimens after the creep elongation in five different alcohols.

strain of 4.7% and subsequent increase to the predetermined value of 9%, exhibiting the curves with upward curvature except the result in ethanol. The creep strain in ethanol noticeably shows a drastic increase with downward curvature in the latter stage. The creep behavior, however, is not clearly correlated with the properties of environmental alcohol given in Table I. For finding some systematic trend of creep deformation against such properties of alcohol, the specimens may be required to be furthermore elongated to the fracture, exceeding the common preset strain of 9%. In this article, therefore, the creep behavior of PA6 in alcohols is not further discussed.

Freezing Behavior of Absorbed Water

Figure 4 shows the DSC cooling curves of water-soaked specimens after the above creep elongation to the strain of 9% in alcohols. All the curves are weight-normalized to a sample weight of 5.0 mg. It is of interest that quite different DSC curves are obtained for the test alcohols in spite of almost the same water content (7.8 or 7.9 wt %, as shown earlier). Several exothermic peaks are clearly observed from −24°C to −33°C for the specimen elongated in ethanol. The smaller exothermic peaks are detected in relatively low temperature range for those in other alcohols, and no peak is found for the specimen in 1-octanol. As mentioned before, the contained water in nondeformed PA6 usually is not frozen at all,[14] as a result of the strong restriction of water molecules to the hydrophilic sites of amide group through the hydrogen bonding.[17] Consequently the absorbed water in the specimen extended in 1-octanol is considered to exist as nonfreezing bound water,[15,16] irrespective of deformation. On the other hand, the exothermic peaks for the specimens elongated in other alcohols are interpreted to indicate the presence of freezable water. According to the preliminary DSC measurement on bulk distilled water under the same condition, the freezing took place at −16.5°C with a sharp exothermic peak, as has been similarly observed in other DSC measurement.[15] Compared with that, the freezing of water at lower temperatures may be basically understood as a manifestation of capillary effect in the voids introduced by the collapse of crystals under large elongation.[1–6] By this effect the freezing temperature of accumulated water in the void is lowered with a decrease in the void size. Based on this understanding, many exothermic DSC peaks observed at different temperatures may mean the existence of voids of various sizes. It is therefore suggested that the creep elongation in ethanol forms some heterogeneous microstructure including a variety of voids, while the elongation in 1-octanol takes place keeping rather homogeneous microstructure without voids.

By the way the heat of freezing of contained water given by the total area under DSC exothermic curves in Figure 4 also may be significant for further discussing the freezing behavior of water itself. In this article, however, as the DSC characterization entirely focuses on the freezing temperature of water required directly for the analysis of thermoporosimetry described below, it is not discussed here.

Assessment of Pore Size Distribution

Based on the above discussion, the void size distribution is evaluated by applying the method of thermoporosimetry to the DSC curves for the specimens elongated in alcohols except 1-octanol. The thermoporosimetry itself has already been explained and examined in detail in the literatures.[7–13] Thus in this article only a short description is given on the procedures using the thermoporosimetry. Hereafter the void is often termed the pore as used in this method.

This article basically follows the method of Ishikiriyama et al.,[7,8] as well as our previous work.[14] According to them, the abscissa and the ordinate of DSC curve of freezable water given in Figure 4 are transformed into the pore radius, R, and the change in the pore volume, dV_p/dR, respectively, by the following equations:

$$R = \frac{\alpha}{\Delta T} = \beta, \tag{1}$$

$$\frac{dV_p}{dR} = \left|\frac{dq}{dt}\right| \frac{dt}{dR} \frac{1}{m\Delta H_m \rho} \frac{R^2}{(R-\beta)^2}, \tag{2}$$

where ΔT is the freezing temperature depression of water in the pore, and α is the inverse proportional coefficient depending on ΔT. Our previous study using this method for PA6 elongated in air[14] has shown the evaluated distributions of pore size to be almost unaffected by the pore shape (cylindrical or spherical). Therefore in this article only the case of cylindrical pore is discussed. For this reason the exponents in eq. (2) are set to 2 (3 in case of spherical pore), and the dependence of α on ΔT is described as α 56.36−0.90ΔT also for the cylindrical pore, as given in Ref. 8. β is the thickness of thin layer of nonfreezable water on the pore surface, where in case of PA6 the water is

strongly caught by the amide group through the hydrogen bonding.[17] As the assembling structure of water molecules bound to the PA pore surface is not clear at present, β is simply set to 0.3 nm corresponding to one molecular size of water approximately estimated from van der Waals radius of 0.14 nm, following the analysis of Kaewnopparat et al.[11] ρ and ΔH_m are the density and the heat of phase transition of freezable pore water, respectively, which are reasonably assumed to be the same as those of bulk water.[7,8]

The pore size distributions calculated by this method are shown in Figure 5. The pores (voids) for the ethanol environment are widely distributed from 2.5 to 8.5 nm in radius (5–17 nm in diameter) showing many peaks of almost the same height, whereas those for 1-propanol and 1-butanol show narrower size distributions from 3 to 4 nm, and further those for 1-hexanol concentrate upon very small size of about 2 nm. Probably similar results of pore size distribution will be obtained for another model of spherical pore, being inferred from the previous study.[14] The pore sizes for alcohols, as a whole, are comparable with or greater than those for air,[14] although an exact comparison may not be done because of a difference in the loading type. The wide pore size distribution for ethanol may correspond to the acceleration in the latter stage of creep. With regards to these pore (void) sizes, they partially exceed the ability of our SEM equipment (Hitachi, S-4000) with a resolution of 1.5 nm at the maximum magnification of ×300,000 (about 5 nm at ×100,000 magnification under usual operation). Thus the SEM observations were not conducted in this article, although the differences between heterogeneous (for ethanol) and homogeneous (for 1-octanol) microstructures are worthy of examinations in detail.

The porosity parameters; the total pore volume, V_p, the internal surface area of pore, S_p, and the average pore radius, R_{ave}, are also calculated from these distributions by the following equations:

$$V_p = \int_0^\infty \left(\frac{dV_p}{dR}\right) dR, \tag{3}$$

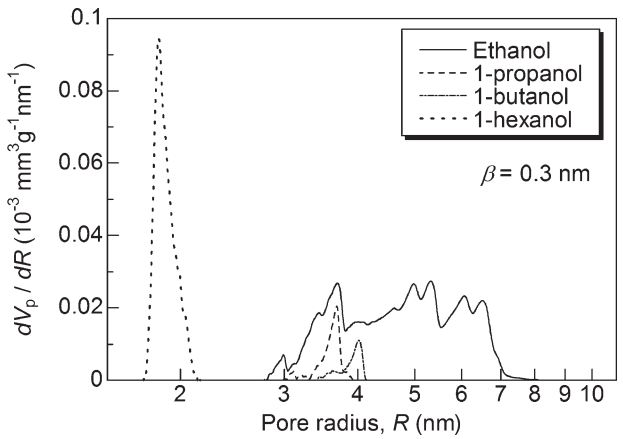

Figure 5. Pore size distributions calculated by the thermoporosimetry for the specimens elongated in five different alcohols.

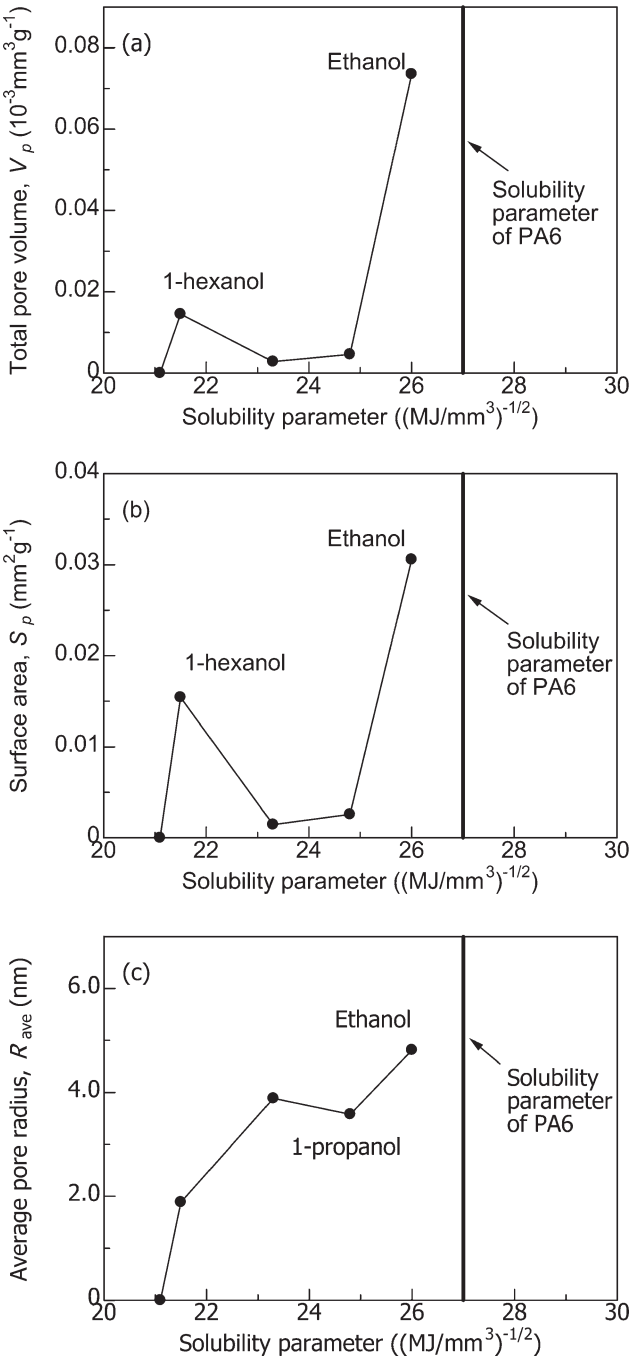

Figure 6. Porosity parameters of the elongated specimens against the solubility parameter of environmental alcohol: (a) the total pore volume, V_p, (b) the surface area, S_p, and (c) the average pore radius, R_{ave}.

$$S_p = \int_0^\infty \frac{2}{R}\left(\frac{dV_p}{dR}\right) dR, \tag{4}$$

$$R_{ave} = \frac{2V_p}{S_p}. \tag{5}$$

The results are shown in Figure 6, where these porosity parameters are plotted against the solubility parameter of alcohol. The solubility parameter of PA6 is denoted by a vertical line at

$27(MJ/m^3)^{1/2}$ in the figure.[29] The porosity parameters, especially the average pore radius, show greater values for alcohols of the solubility parameter near that of PA6. This trend suggests the solubility of environmental alcohol to actively participate in the formation and expansion of voids during the creep elongation. The result in ethanol may be mostly adequate to this suggestion. In the cases of the total volume and the internal surface area of pore, the result for 1-hexanol greatly deviates from this trend, probably reflecting some peculiarity in the pore size distribution indicated in Figure 5. In 1-hexanol many small voids are formed, but may hold their initial sizes during the deformation, although the reason is not clear at present. It may be hypothesized, as a whole, that the alcohols with different solubility parameters induce different levels of plasticization of PA6 leading to various pore (void) sizes and their distributions.

As regards the above discussion, however, it is reminded that the formation of craze including many voids is not always correlated with the solubility parameter of environmental reagent. Kawagoe et al.[30–32] have revealed that both the critical stress and strain for crazing in amorphous glassy polymers are not correlated with the solubility parameter, nor with the equilibrium solubility, and rather with the absorption (diffusion) rate of reagent. Therefore further examinations may be required on the relationship between the present results of pore size distribution in the deformed PA6 and the absorption behavior of environmental alcohol. In addition, it also may be of interest to consider as a future subject the variations of crystalline microstructure like the degree of crystallinity with the creep in different alcohols in relation to their solubility and absorption behavior. In this connection, as the degree of penetration and thus influence of environmental reagent on the void formation may vary with the depth from the surface, repeating this thermoporosimetric measurement for each thin layer will supply some three-dimensional information of voided microstructure formed under the action of reagent.

Thus the use of thermoporosimetry may be proposed for a novel approach to the characterization of void formation in the plastically deformed polymers. Compared with other methods like electron microscopy (SEM and TEM) and SAX measurements, this method may not specify the location, shape, and exact size (aspect ratio) of each void, but seems to have an advantage to evaluate the size distribution of numerous voids over much larger volume in the deformed region by one time measurement. This feature may be especially beneficial for making a relative comparison between different specimens, as indicated in this article.

CONCLUSIONS

The void formation in PA6 developed under the creep tensile loading in five different alcohols was characterized by using the thermopolosimetry based on the DSC cooling analyses of absorbed water in the deformed specimens. Irrespective of the kind of test alcohol, similar results of creep deformation were observed until a preset strain of 9%, except in ethanol. The specimen in ethanol noticeably showed a drastic increase in strain in the latter stage of creep. These creep-deformed specimens were soaked in distilled water, and subsequently offered to the DSC measurements under cooling condition. Several exothermic peaks indicating the presence of freezable water were evidently observed at lower temperatures than bulk water for the specimens deformed in alcohols except 1-octanol. Especially the specimen elongated in ethanol showed many exothermic peaks in wide range of temperature. Considering the capillary effect on the water freezing, these results were interpreted to mean the existence of voids of various sizes, which were formed during the creep deformation in alcohols.

Based on this interpretation, the size distributions of void were assessed from the DSC curves of water freezing by the means of thermoporosimetry for a model of cylindrical pore. The pores for the ethanol environment showed a wide size distribution, probably corresponding to the creep acceleration in the latter stage. The pores for 1-propanol and 1-butanol showed narrower size distributions, and those for 1-hexanol concentrated upon very small size. The average pore radius was increased, as the solubility parameter of environmental alcohol approached that of PA6. This result suggests the solubility of environmental alcohol to participate in the formation and expansion of voids during the creep elongation, particularly in ethanol. However, besides the solubility properties, the absorption behavior of environmental alcohol also should be examined in relation to the pore size distribution.

ACKNOWLEDGMENTS

The authors wish to thank Associate Professor K. Sanada, Toyama Prefectural University, for valuable discussions.

REFERENCES

1. Friedrich, K. In Crazing in Polymers; Kausch, H. H., Ed.; Springer-Verlag: Berlin, **1983**; p 225.
2. Butler, M. F.; Donald, A. M.; Ryan, A. J. *Polymer* **1997**, *38*, 5521.
3. Butler, M. F.; Donald, A. M.; Ryan, A. J. *Polymer* **1998**, *39*, 39.
4. Galeski, A.; Argon A. S.; Cohen, R. E. *Macromolecules* **1988**, *21*, 2761.
5. Pawlak, A.; Galeski, A. *Macromolecules* **2005**, *38*, 9688.
6. Li, J. X.; Cheung, X. L.; Chan, C. M. *Polymer* **1999**, *40*, 3641.
7. Ishikiriyama, K.; Todoki, M.; Motomura, K. *J. Colloid Interface Sci.* **1995**, *171*, 92.
8. Ishikiriyama, K.; Todoki, M. *J. Colloid Interface Sci.* **1995**, *171*, 103.
9. Luukkonen, P.; Maloney, T.; Rantanen, J.; Paulapuro, H.; Yliruusi, J. *Pharm. Res.* **2001**, *18*, 1562.
10. Faroongsarng, D.; Peck, G.E. *AAPS PharmSciTech* **2003**, *4*, 1.
11. Kaewnopparat S.; Sansernluk, K.; Faroongsarng, D. *AAPS PharmSciTech* **2008**, *9*, 701.
12. Iijima, M.; Sasaki, Y.; Osada, T.; Miyamoto, K.; Nagai, M. *Int. J. Thermophys.* **2006**, *27*, 1792.

13. Nedelec, J-M; Grolier, J-P.E.; Baba, M. *J. Sol-Gel Sci. Technol.* **2006**, *40*, 191.
14. Sakai, E.; Kawagoe, M. *J. Appl. Polym. Sci.* **2010**, *115*, 1272.
15. Nakamura, K.; Hatakeyama, T.; Hatakeyama, H. *Polymer* **1983**, *24*, 871.
16. Higuchi,A.; Iijima, T. *Polymer* **1985**, *26*, 1207.
17. Fukumoto, O. Polyamide Resin Handbook; Nikkan Kougyou Shinbunsha: Tokyo, **1988**; Chapter 5, p 86 (in Japanese).
18. Kausch, H.H. Polymer Fracture; Springer-Verlag: Berlin, **1978**; Chapter 8, p 193.
19. Andrews, E.H.; Reed, P.E. In Developments in Polymer Fracture-1; Andrews, E. H., Ed.; Applied Science Publishers: London, **1979**; Chapter 2, p 48.
20. Kramer, E.J. In Developments in Polymer Fracture-1; Andrews, E. H., Ed.; Applied Science Publishers: London, **1979**; Chapter 3, p 55.
21. Kramer, E.J. In Developments in Polymer Fracture-1; Andrews, E. H., Ed.; Applied Science Publishers: London, **1979**; Chapter 3, p 69.
22. Kinloch, A.J.; Young, R.J. In Fracture Behaviour of Polymers; Applied Science Publishers: London, **1979**; Chapter 9, p 354.
23. Maxwell, A.S. NPL Report DEPC MPR 015; National Physical Laboratory: Teddington, UK, **2005**, p 7.
24. In JIS Handbook-Plastic; Japanese Industrial Standards Association: Tokyo, 1992; p 331 (in Japanese).
25. Miller, R. L. In Polymer Handbook; Brandrup, J.; Immergut, E.H., Eds.; Wiley-Interscience: New York, **1975**; p III-25.
26. In Wako CHEMICALS; Wako Pure Chemical Industries, Ltd.: Osaka, 2012 (in Japanese).
27. In Youzai Handbook; Asahara, T.; Tokura, N.; Ookawara, M.; Kumanotani, J.; Senoo, S., Eds; Kodansha: Tokyo, **1976** (in Japanese).
28. Barton, A. F. M. *Chem. Rev.* **1975**, *75*, 731.
29. Burrell, H. In Polymer Handbook; Brandrup, J.; Immergut, E.H., Eds; Wiley-Interscience: New York, **1975**, p IV-351.
30. Kawagoe, M; Ishimi, T. *J. Mater. Sci.* **2002**, *37*, 5115.
31. Kawagoe, M; Kitagawa, M. *J. Mater. Sci.* **1987**, *22*, 3000.
32. Kawagoe, M; Morita, M. *J. Mater. Sci.* **1994**, *29*, 6041.